Substituent Effects on the Choice of the Orbital Preferred for Electron Spin Delocalization in Two Paramagnetic Low-Spin Iron(III) Porphyrins: Mapping the Spin Density Distribution at the Pyrrole Positions by ^{1}H COSY and NOESY Techniques

Helming Tan,[†] Ursula Simonis,*[,†] Nikolai V. Shokhirev,*[,‡,1] and F. Ann Walker*[,‡]

Contribution from the Department of Chemistry and Biochemistry, San Francisco State University, San Francisco, California 94132, and Department of Chemistry, University of Arizona, Tucson, Arizona 85721

Received September 8, 1993[⊕]

Abstract: In order to elucidate the distribution of unpaired electron spin density within the porphyrin π orbitals of two unsymmetrically substituted derivatives of (tetraphenylporphyrinato)iron(III), [(*p*-Cl)(*p*-NEt_2)$_3$TPPFe(*N*-MeIm)$_2$]-Cl and [(*p*-NEt_2)(*p*-Cl)$_3$TPPFe(*N*-MeIm)$_2$]Cl (NEt_2 = diethylamino; *N*-MeIm = *N*-methylimidazole), ^{1}H COSY and NOESY spectra were acquired. The cross peak patterns observed in the 2-D maps of these complexes allow assignment of the proton resonances in the same pyrrole ring (H_a,H_b and H_c,H_d) and of those that are closest to each other in adjacent pyrrole rings (H_b,H_c). Using these assignments, it is possible to delineate the pattern of unpaired electron spin delocalization in the porphyrin ring. This pattern can be unambiguously correlated to the relative electronic effects of the two types of phenyl substituents present, thereby permitting the electron-donating or -withdrawing effects of other substituents to be predicted. In order to test if the pattern of delocalized spin density derived from the 2-D NMR studies can be modeled, simple Hückel molecular orbital calculations were performed. Although only intended to provide a qualitative understanding of the effects of electron-donating and -withdrawing substituents, these most basic calculations provided significant results. Using well-established Hückel parameters, together with lowering or raising the energy of the p_z orbital of one *meso*-carbon atom to account for the electronic nature of the unique substituent, an electron density distribution was obtained that fully supports the ^{1}H resonance assignments based on the cross peaks observed in the COSY and NOESY maps of these complexes. This indicates that more sophisticated theoretical calculations may lead to a quantitative description of the effects of porphyrin substituents on the pattern of spin delocalization in synthetic and naturally occurring hemes and their byproducts. In support of this conclusion, it should be noted that even the simplest Hückel calculations described herein have already proved valuable in explaining the pattern of spin delocalization observed in the substrate-bound form of the enzyme heme oxygenase, which catalyzes the stereospecific α-*meso* bridge cleavage of hemin to yield biliverdin-IXα (Hernández, G.; Wilks, A.; Paolesse, R.; Smith, K. M.; Ortiz de Montellano, P. R.; La Mar, G. N. *Biochemistry*, in press).

Introduction

We and others have shown that ^{1}H NMR spectroscopy is a powerful technique for determining structure–function relationships of the active sites of heme proteins[2-14] and model hemes[15-33] and for obtaining detailed information concerning the local heme

† San Francisco State University.
‡ University of Arizona.
⊕ Abstract published in *Advance ACS Abstracts*, May 15, 1994.

(1) Permanent address: Institute of Chemical Kinetics and Combustion, Russian Academy of Sciences, Novosibirsk 630090, Russia.

(2) La Mar, G. N. In *Biological Applications of Magnetic Resonance*; Shulman, R. B., Ed.; Academic Press: New York, 1979; p 305.

(3) (a) Satterlee, J. D. *Annu. Rep. NMR Spectrosc.* **1986**, *17*, 79. (b) Satterlee, J. D. In *Metal Ions in Biological Systems*; Sigel, H., Ed.; Marcel Dekker: New York, 1986; Vol. 21, p 121.

(4) La Mar, G. N.; de Ropp, J. S. In *Biological Magnetic Resonance*; Berliner, L. J., Reuben, J., Eds.; Plenum Press: New York, 1993; Vol. 12, pp 1–73.

(5) (a) Concar, W.; Whitford, D.; Williams, R. J. P. *Eur. J. Biochem.* **1991**, *199*, 569; (b) *FEBS Lett.* **1990**, *269*, 297; (c) *Biomol. NMR* **1991**, *353*, 6343.

(6) Peyton, D. H. *Biochem. Biophys. Res. Commun.* **1991**, *175*, 517.

(7) Timkovich, R. *Inorg. Chem.* **1991**, *30*, 37; *Biochemistry* **1993**, *32*, 11516.

(8) Morikis, D.; Bruschweiler, R.; Wright, P. E. *J. Am. Chem. Soc.* **1993**, *115*, 6238.

(9) (a) Coutinho, J. B.; Turner, D. L.; LeGall, J.; Xavier, A. V. *Eur. J. Biochem.* **1992**, *209*, 329. (b) Santos, H.; Turner, D. L. *Ibid.* **1992**, *206*, 721. (c) Turner, D. L.; Williams, R. J. P. *Ibid.* **1993**, *211*, 555. (d) Turner, D. L. *Ibid.* **1993**, *211*, 563; (e) *Ibid.* **1993**, *215*, 817.

(10) Satterlee, J. D.; Alam, S.; Yi, Q.; Erman, J. E.; Constantinidis, I.; Russell, D. J.; Moench, S. J. In *Biological Magnetic Resonance*; Berliner, L. J., Rueben, J., Eds.; Plenum Press: New York, 1993; Vol. 12, pp 275–297.

(11) (a) Yamamoto, Y. *Biochem. Biophys. Res. Commun.* **1993**, 4196, 348. (b) Yamamoto, Y.; Suzuki, T. *Biochim. Biophys. Acta* **1993**, *1163*, 287.

(12) McLachlan, S. J.; La Mar, G. N.; Lee, K.-B. *Biochim. Biophys. Acta* **1988**, *957*, 430.

(13) (a) Ishimori, K.; Imai, K.; Miyazaki, G.; Kitagawa, T.; Wada, Y.; Morimoto, H.; Morishima, I. *Biochemistry* **1992**, *31*, 3256. (b) Adachi, S.; Nagano, S.; Ishimori, K.; Watanabe, Y.; Morishima, I.; Egawa, T.; Kitagawa, T.; Makino, R. *Biochemistry* **1993**, *32*, 241.

(14) (a) Bertini, I.; Luchinat, C. In *NMR of Paramagnetic Molecules in Biological Systems*; Bowen, D. L., Hubit, G., Myson-Etherington, D., Eds.; Benjamin/Cummings: Menlo Park, CA 1986. (b) Banci, L.; Bertini, I.; Luchinat, C. In *Nuclear and Electron Relaxation*; Weller, M. G., Maier, H. J., Eds.; VCH: Weinheim, 1991.

(15) La Mar, G. N.; Walker, F. A. NMR Studies of Paramagnetic Metalloporphyrins. In *The Porphyrins*; Dolphin, D., Ed.; Academic Press: New York, 1979; Vol. IV, pp 61–157.

(16) Goff, H. M. In *Iron Porphyrins*; Lever, A. B. P., Gray, H. B., Eds.; Addison-Wesley: Reading, MA, 1983; Part I, pp 239–281.

(17) Walker, F. A.; Simonis, U. Proton NMR Spectroscopy of Model Hemes. In *Biological Magnetic Resonance: NMR of Paramagnetic Molecules*; Berliner, L. J., Ruben, J., Eds.; Plenum Press: New York, 1993; Vol. 12, pp 133–274.

(18) (a) Yamamoto, Y.; Fujii, H. *Chem. Lett. Jpn.* **1987**, 1703. (b) Yamamoto, Y.; Nanai, N.; Chujo, R.; Suzuki, T. *FEBS Lett.* **1990**, *264*, 113. (c) Yamamoto, Y.; Chujo, R.; Suzuki, T. *Eur. J. Biochem.* **1991**, *198*, 285.

(19) (a) Yamaguchi, K.; Morishima, I. *Inorg. Chem.* **1992**, *31*, 3216. (b) Ozawa, S.; Fujii, H.; Morishima, I. *J. Am. Chem. Soc.* **1992**, *114*, 1548.

(20) Unger, S. W.; Jue, T.; La Mar, G. N. *J. Magn. Reson.* **1985**, *61*, 448.

(21) (a) Nakamura, M. *Chem. Lett. Jpn.* **1988**, 453. (b) Nakamura, M. *Inorg. Chim. Acta* **1989**, *161*, 73. (c) Nakamura, M.; Nakamura, N. *Chem. Lett. Jpn.* **1990**, 181.

(22) Walker, F. A.; Simonis, U.; Zhang, H.; Walker, J. M.; Ruscitti, T. M.; Kipp, C.; Amputch, M. A.; Castillo, B. V.; Cody, S. H.; Wilson, D. L.; Graul, R. E.; Yong, G. J.; Tobin, K.; West, J. T.; Barichievich, B. A. *New J. Chem.* **1992**, *16*, 609.

(23) Nakamura, M.; Groves, J. T. *Tetrahedron* **1988**, *44*, 3225.

(24) Walker, F. A.; Simonis, U. *J. Am. Chem. Soc.* **1991**, *113*, 8652.

0002-7863/94/1516-5784$04.50/0

environment. In particular, the hyperfine-shifted ^{1}H resonances of the heme group have been used as a probe for characterizing the heme electronic environment.[15,17-20] Proton NMR spectroscopy has also been successfully utilized for studying such effects as dynamics of axial ligand binding[15,17,21,22] and rotation,[22-25] T_1 and T_2 relaxation processes,[14,16,20] and for mapping the spin density distribution around the porphyrin skeleton.[15-17] Although only 15–20% of the unpaired electron of low-spin Fe(III) is delocalized onto the porphyrin ring, the protons directly attached to or closest to the eight β-pyrrole carbons of the porphyrin macrocycle exhibit large paramagnetic shifts which "illuminate" the porphyrin substituents and thereby serve as ideal tools for investigating the electronic properties of the heme moiety, especially for determining the spin density distribution around the porphyrin skeleton[15,17,20] and the factors that modify it. Quantitative understanding of this unpaired electron spin density distribution is vital for understanding the reactivities of both the metal and the porphyrin ring in heme proteins.

Since the use of ^{1}H NMR spectroscopy for obtaining a simple description of the π electron density distribution within the porphyrin macrocycle of heme proteins is made more complex by the combined effects of the low symmetry of the substituent pattern of naturally occurring hemes, the large effect of histidine or methionine π-symmetry lone pair orientation,[3b,12,34] and the less quantifiable effect of protein side chains pressing against certain portions of the heme ring,[3b,35] we have turned to the investigation of higher-symmetry model hemes, in order to determine unequivocally the factors that affect the pattern of unpaired electron delocalization through the porphyrin π orbitals in both model hemes and heme proteins.[15,17,22,26-33] Paramagnetic, low-spin (porphyrinato)iron(III) complexes are ideal candidates for these investigations, since the hyperfine shift patterns of the model iron porphyrins[15-19] and the intact heme proteins[2-12] parallel each other. Hence, as pointed out by La Mar et al.[36] and Turner,[9e] these simple complexes are excellent models for elucidating protein-based perturbations.

Furthermore, low-spin derivatives of (tetraphenylporphyrinato)iron(III) can be easily synthesized to introduce varying degrees of asymmetry into the π electronic system of the porphyrin ring by placing a unique substituent on one of the phenyl rings. Even though the phenyl rings of tetraphenylporphyrins (TPPs) and their metal complexes are, on average, perpendicular to the plane of the porphyrin ring and are thus only very weakly coupled to it through resonance,[37] the inductive effect of the unique substituent is sufficient to cause redistribution of the π electron density and hence also the delocalized unpaired electron spin density at the tetrapyrrole periphery,[36] which is measured by the pattern of the pyrrole proton resonance shifts.[22,25-28,30-33] In order to clearly delineate the electronic effects of substituents on the pattern of spin delocalization within the porphyrin macrocycles of both natural and model hemes, it is therefore essential to completely or even partially assign the pyrrole proton resonances.

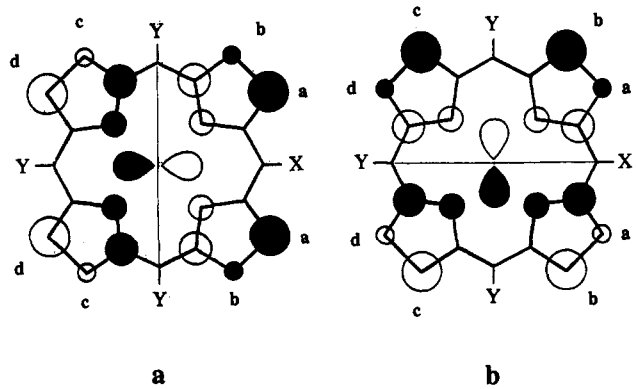

Figure 1. The degenerate filled 3e(π) orbitals of a symmetrically substituted porphyrin ring and the d_π orbital with which each one interacts. The porphyrin orbitals shown are linear combinations of those presented previously,[40c,45,46] since the complexes of the present study contain *meso*-substituted rather than pyrrole-substituted porphyrins.

However, at present only a few reports of such assignments have been described.[17,32,36,38-41]

We have recently used homonuclear correlation spectroscopy (COSY)[42-44] to determine which protons belong to the same pyrrole ring in three unsymmetrically substituted (tetraphenylporphyrinato)iron(III) bis(*N*-methylimidazole) complexes,[30] [(*o*-Cl)(*p*-OCH$_3$)$_3$TPPFe(*N*-MeIm)$_2$]$^+$, [(*o*-COOH)TPPFe(*N*-MeIm)$_2$]$^+$, and [(*o*-OEt)TPPFe(*N*-MeIm)$_2$]$^+$. The COSY cross peaks of these three complexes are consistent with the pattern of spin delocalization at the β-pyrrole positions predicted by a model developed earlier by this group.[26,27,30] This model first considers the electron density distribution in the filled 3e(π) porphyrin orbitals,[45,46] shown in Figure 1, that have the proper symmetry for overlap with the d_π orbitals, d_{xz} and d_{yz}, of low-spin Fe(III). For a symmetrically substituted porphyrin, X = Y, and the two e-symmetry orbitals created by this overlap are degenerate. By placing the nodal planes at the meso positions, the electron density distribution is large-small within each pyrrole ring, or $\rho_{Ca} = \rho_{Cd} \gg \rho_{Cb} = \rho_{Cc}$ for the orbital of Figure 1a and $\rho_{Ca} = \rho_{Cd} \ll \rho_{Cb} = \rho_{Cc}$ for that of Figure 1b. Formation of molecular orbitals by interaction of these porphyrin e(π) and metal d_π orbitals produces a low-energy set that is mainly porphyrin in character and a high-energy (valence) set that is mainly metal in character; the electron configuration is $(e)^3$ in this symmetrical system. However, if the symmetry of the system is lowered by introducing one unique meso substituent (X $\neq$ Y), the two e-symmetry valence molecular orbitals will no longer be degenerate, and their electron density distribution will be modified slightly by the electron-donating/withdrawing characteristics of the substituent attached to the unique phenyl ring.[26,27,30] On the basis of this model, it was possible to predict the scalar coupling pattern expected among the four pyrrole proton resonances observed. However, with only COSY data available, it was not possible to choose of the two

(25) Zhang, H.; Simonis, U.; Walker, F. A. *J. Am. Chem. Soc.* **1990**, *112*, 6124.
(26) Walker, F. A. *J. Am. Chem. Soc.* **1980**, *102*, 3254.
(27) Walker, F. A.; Benson, M. *J. Phys. Chem.* **1982**, *86*, 3495.
(28) Walker, F. A.; Balke, V. L.; McDermott, G. A. *J. Am. Chem. Soc.* **1982**, *104*, 1569.
(29) Walker, F. A.; Buehler, J.; West, J. T.; Hinds, J. L. *J. Am. Chem. Soc.* **1983**, *105*, 6923.
(30) Lin, Q.; Simonis, U.; Tipton, A. R.; Norvell, C. J.; Walker, F. A. *Inorg. Chem.* **1992**, *31*, 4216.
(31) Simonis, U.; Walker, F. A.; Lin, Q. *J. Cell Biochem.* **1993**, *17C*, 301.
(32) Isaac, M. F.; Lin, Q.; Simonis, U.; Suffian, D. J.; Wilson, D. L.; Walker, F. A. *Inorg. Chem.* **1993**, *32*, 4030.
(33) Simonis, U.; Lin, Q.; Tan, H.; Barber, R. A.; Walker, F. A. *Magn. Reson. Chem.* **1993**, *31*, S133.
(34) Keller, R. M.; Schejter, A.; Wüthrich, K. *Biochim. Biophys. Acta* **1980**, *626*, 15.
(35) Lee, K.-B.; La Mar, G. N.; Kehres, L. A.; Fujinari, E. M.; Smith, K. M.; Pochapsky, T. C.; Sligar, S. G. *Biochemistry* **1990**, *29*, 9623.
(36) Keating, K. A.; De Ropp, J. S.; La Mar, G. N.; Balch, A. L.; Shaiu, F. Y.; Smith, K. M. *Inorg. Chem.* **1991**, *30*, 3258.
(37) Balke, V. L.; Walker, F. A.; West, J. T. *J. Am. Chem. Soc.* **1985**, *107*, 1226.
(38) Yu, C.; Unger, S. W.; La Mar, G. N. *J. Magn. Reson.* **1986**, *67*, 346.
(39) Bondoc, L. L.; Chau, M.-H.; Price, M. A.; Timkovich, R. *Biochemistry* **1986**, *25*, 8458.
(40) (a) Chatfield, M. J.; La Mar, G. N.; Lecomte, J. T. J.; Balch, A. L.; Smith, K. M.; Langry, K. C. *J. Am. Chem. Soc.* **1986**, *108*, 7108. (b) Chatfield, M. J.; La Mar, G. N.; Kauten, R. J. *Biochemistry* **1987**, *26*, 6939. (c) Chatfield, M. J.; La Mar, G. N.; Parker, W. O.; Smith, K. M.; Leung, H.-K.; Morris, I. K. *J. Am. Chem. Soc.* **1988**, *110*, 6352.
(41) Liacoccia, S.; Chatfield, M. J.; La Mar, G. N.; Smith, K. M.; Mansfield, K. E.; Anderson, R. R. *J. Am. Chem. Soc.* **1989**, *111*, 6087.
(42) Croasmun, W. R.; Carlson, R. M. K. In *Two-Dimensional NMR Spectroscopy. Applications for Chemists and Biochemists*; Marchand, A. P., Ed.; VCH Publishers: New York, 1987.
(43) Martin, G. E.; Zektzer, A. S. In *Two-Dimensional NMR Methods for Establishing Molecular Connectivity*; Marchand, A. P., Ed.; VCH Publishers: New York, 1988.
(44) Bax, A. *Two-Dimensional Nuclear Magnetic Resonance in Liquids*; D. Reidel Publishing Co.: Dordrecht, The Netherlands, 1984.
(45) Longuet-Higgins, H. C.; Rector, C. W.; Platt, J. R. *J. Chem. Phys.* **1950**, *18*, 1174.
(46) Gouterman, M. In *The Porphyrins*; Dolphin, D., Ed.; Academic Press: New York, 1978; Vol. 3, pp 1–165.

e-symmetry valence molecular orbitals created from the substituent-modified versions of those shown in Figure 1 the one preferred for spin delocalization. Furthermore, our representations of the modified molecular orbitals were only pictorial, and, in addition, we were not able to predict the electronic nature of ortho substituents, *i.e.*, whether they are electron-donating or electron-withdrawing. NOESY investigations of some of the same complexes have pointed out the problems associated with the unambiguous assignment of the orbital preferred for spin delocalization in ortho-substituted $[TPPFe(N\text{-}MeIm)_2]^+$ complexes and the difficulty in understanding the electronic effects of ortho substituents.[33]

The challenges encountered with $[TPPFe(N\text{-}MeIm)_2]^+$ derivatives containing ortho substituents have led us to reinvestigate[28] two unsymmetrically *p*-phenyl-substituted complexes, $[(p\text{-}Cl)(p\text{-}NEt_2)_3TPPFe(N\text{-}MeIm)_2]Cl$ (**1**) and $[(p\text{-}NEt_2)(p\text{-}Cl)_3TPPFe(N\text{-}MeIm)_2]Cl$ (**2**) (NEt_2 = diethylamino; *N*-MeIm = *N*-methylimidazole), for which the electronic nature of the para substituents is well documented.[47] In this paper we will discuss in detail how homonuclear correlated (COSY)[42-44] and homonuclear Overhauser enhancement (NOESY)[48] spectroscopy performed for **1** and **2** provide key steps in addressing the relationship between the electron-donating or -withdrawing nature of the para substituent and the unpaired electron spin delocalization pattern in the valence e-symmetry molecular orbitals derived from those shown in Figure 1. In addition, we will demonstrate that even the most basic types of Hückel calculations[49,50] allow us to model the effect of substituents on the electron density distribution within the porphyrin macrocycle and hence allow us to predict the relative resonance shifts of the pyrrole protons. The results of these simple computations thus clearly indicate the potential of more sophisticated calculations to provide a quantitative description of the effect of substituents. Finally, we will show that the combination of even partial assignment of the pyrrole proton resonances by COSY and NOESY techniques and modeling by even the simplest molecular orbital techniques can not only be used to develop an approach for predicting the assignments of the hyperfine-shifted resonances of model hemes and heme proteins but also can lead and has already led to predictions concerning the mechanism of reaction at the heme periphery of the enzyme heme oxygenase.[51,52] This combination may also be of value for investigating structure–function relationships in other heme proteins, such as the effect of heme substituents in the nature of the π molecular orbital used for unpaired electron spin delocalization in cytochrome P450.[53]

Experimental Section

The free base porphyrins $[(p\text{-}Cl)(p\text{-}NEt_2)_3TPPH_2]$ and $[(p\text{-}NEt_2)_1(p\text{-}Cl)_3TPPH_2]$ were prepared previously[54] and were purified by column chromatography on silica gel (Fisher Scientific) using toluene as eluting solvent. Iron was inserted, and the chloroiron(III) complexes **1** and **2** were purified as described previously.[28] The *N*-methylimidazole (*N*-MeIm) complexes were prepared in the NMR tube by dissolving the high-spin chloroiron(III) complexes in CD_2Cl_2 and adding aliquots of *N*-MeIm until no resonances of the high-spin Fe(III) complex were detectable.

Magnitude COSY-45 spectra of **1** and **2** were acquired as reported previously.[30] Homonuclear Overhauser and chemical exchange spectroscopy (NOESY) experiments[48] for **1** and **2** were recorded in CD_2Cl_2 at −35 °C on a General Electric GN-300 NMR spectrometer as described elsewhere.[33] The low temperature was chosen because it was found that chemical exchange of the axial ligands was very slow on the NMR time scale at that temperature. NOESY spectra were acquired using either 64 or 128 t_1 data points of 64–256 scans each over a bandwidth of 8.8 kHz and 256 or 512 t_2 data points. The data sets were obtained utilizing the $[90°\text{–}t_1\text{–}90°\text{–}(\tau_m+\chi t_1)/2\text{–}180°\text{–}(\tau_m-\chi t_1)/2\text{–}90°\text{–}t_2]$ pulse sequence, with the composite 180° pulse applied during the mixing period, which, in combination with symmetrization of the final data set, suppresses cross correlations due to scalar couplings.[55] Recycle delays of either 200 or 300 ms were used. The mixing times were systematically varied from 2 to 20 ms to determine which resulted in maximum cross peak intensity, which was usually obtained when the mixing time was chosen to be 15–30% longer than the shortest T_1 of the protons of interest. Data were processed with an unshifted sine-bell window function in both dimensions, zero-filled once or twice to give final matrices of $256t_1 \times 256t_2$ or $512t_1 \times 512t_2$ data points prior to Fourier transformation, magnitude calculation, and symmetrization.

The electron densities in the π molecular orbitals were calculated using simple Hückel molecular orbital theory.[45,49,50] The only differences between our treatment and that of Longuet-Higgins *et al.*[45] are that (a) we have used the accepted[49] Coulomb integral for nitrogen, rather than considering it to be identical to that of carbon, and (b) we have included the *metal d_π orbitals* in the calculations. Standard values for the Coulomb integrals (in units of $|\beta_{CC}|$) α_C (0.0),[49] α_N (−0.5),[49] and α_{Fe} (−0.2)[50] were taken from the literature, except as mentioned below. The resonance integrals β_{CN} ($-0.8|\beta_{CC}|$)[49] and β_{FeN} ($-0.2|\beta_{CC}|$)[50] used in this work are also standard values. The inductive effect of the electron-donating or -withdrawing substituent was simulated by raising or lowering the energy of one *meso*-carbon p_π orbital, respectively. Such empirical adjustment of the energy of a carbon p_π orbital to simulate the inductive effect of an electron-donating or -withdrawing substituent has been done by previous workers.[49] It was found that satisfactory modeling of the contact shift patterns of complex **1** and **2** could be achieved by decreasing α_C for *meso*-C_5 to $-0.3|\beta_{CC}|$ for **1** and by increasing α_C to $+0.15|\beta_{CC}|$ for **2**. Because C_5 lies on a node of one of the two π orbitals of interest (Figure 1b), additional improvement was achieved by lowering or raising the energies of the α-carbons adjacent to *meso*-C_5 (i.e., C_4 and C_6) for **1** and **2**, respectively, by one-tenth the amount by which the energy of *meso*-C_5 was adjusted in each case. (This is equivalent to considering that the inductive effect of the *meso*-C_5 substituent extends as far as C_4 and C_6, but to a greatly diminished extent.) Neither adjustment in the energies of the *meso*-C_5 crbon nor adjustment in the adjacent α-carbons C_4 and C_6 changed the energy of the orbital of Figure 1b, while the energy of the orbital of Figure 1a was shifted up when the energy of *meso*-C_5 (and C_4 and C_6) was adjusted up and down when it was adjusted down. Calculated simple Hückel MO coefficients are presented in Table SI, and a semiquantitative comparison of contact shifts and Hückel MO coefficients is presented in Table SII (supplementary material).

Results and Discussion

Complexes **1** and **2**, shown in Figures 2a and 3a, respectively, which contain one electron-withdrawing (Cl) or one electron-donating $(NEt)_2$ substituent at the para position of one phenyl ring, respectively, relative to the other three *p*-phenyl substituents, are ideal candidates for investigating the nature of spin delocalization within the porphyrin macrocycle and for understanding unambiguously the relationship between the electronic properties of the substituents and the shape of the porphyrin $3e(\pi)$ orbital preferred for spin delocalization in low-spin Fe(III) derivatives. The electronic effects of the *p*-phenyl substituents are well understood for these two complexes, *i.e.*, the *p*-NEt_2 substituent is clearly electron-donating (Hammett $\sigma = -0.83$[47]), whereas the *p*-Cl substituent is electron-withdrawing ($\sigma = +0.227$[47]).

(47) Leffler, J. E.; Grunwald, E. *Rates and Equilibria of Organic Reactions*; Wiley: New York, 1963; pp 172–173. Swain, C. G.; Lupton, E. C. *J. Am. Chem. Soc.* **1968**, *90*, 4328. Ehrenson, S.; Brownlee, R. T. C.; Taft, R. W. *Prog. Phys. Org. Chem.* **1973**, *10*, 1.

(48) Neuhaus, D.; Williamson, M. P. *The Nuclear Overhauser Effect in Structural And Conformational Analysis*; VCH Publishers: New York, 1989.

(49) Streitwieser, A., Jr. *Molecular Orbital Theory for Organic Chemists*; John Wiley: New York, 1961.

(50) Greenwood, H. H. *Computing Methods in Quantum Organic Chemistry*; Wiley-Interscience: New York, 1972.

(51) (a) Schmid, R.; McDonagh, A. F. In *The Porphyrins*; Dolphin, D., Ed.; Academic Press: New York, 1979; Vol. VI, pp. 257–292. (b) Frydman, R. B.; Frydman, B. *Acc. Chem. Res.* **1987**, *20*, 250.

(52) Hernández, G.; Wilks, A.; Paolesse, R.; Smith, K. M.; Ortiz de Montellano, P. R.; La Mar, G. N. *Biochemistry*, in press.

(53) (a) Banci, L.; Bertini, I.; Marconi, S.; Pierattelli, R. *Eur. J. Biochem.* **1993**, *215*, 431. (b) Banci, L.; Bertini, I.; Eltis, L. D.; Pierattelli, R. *Biophys. J.* **1993**, *65*, 806. (c) Tuck, S. F.; Graham-Lorence, S.; Peterson, J. A.; Ortiz de Montellano, P. R. *J. Biol. Chem.* **1993**, *268*, 269.

(54) Walker, F. A.; Balke, V. L.; McDermott, G. A. *Inorg. Chem.* **1982**, *21*, 3342.

(55) (a) Jeener, J.; Meier, B. H.; Bachmann, P.; Ernst, R. R. *J. Phys. Chem.* **1979**, *71*, 4546. (b) Macura, S.; Wüthrich, K.; Ernst, R. R. *J. Magn. Reson.* **1982**, *46*, 269. (c) Macura, S.; Wüthrich, K.; Ernst, R. R. *J. Magn. Reson.* **1982**, *47*, 351.

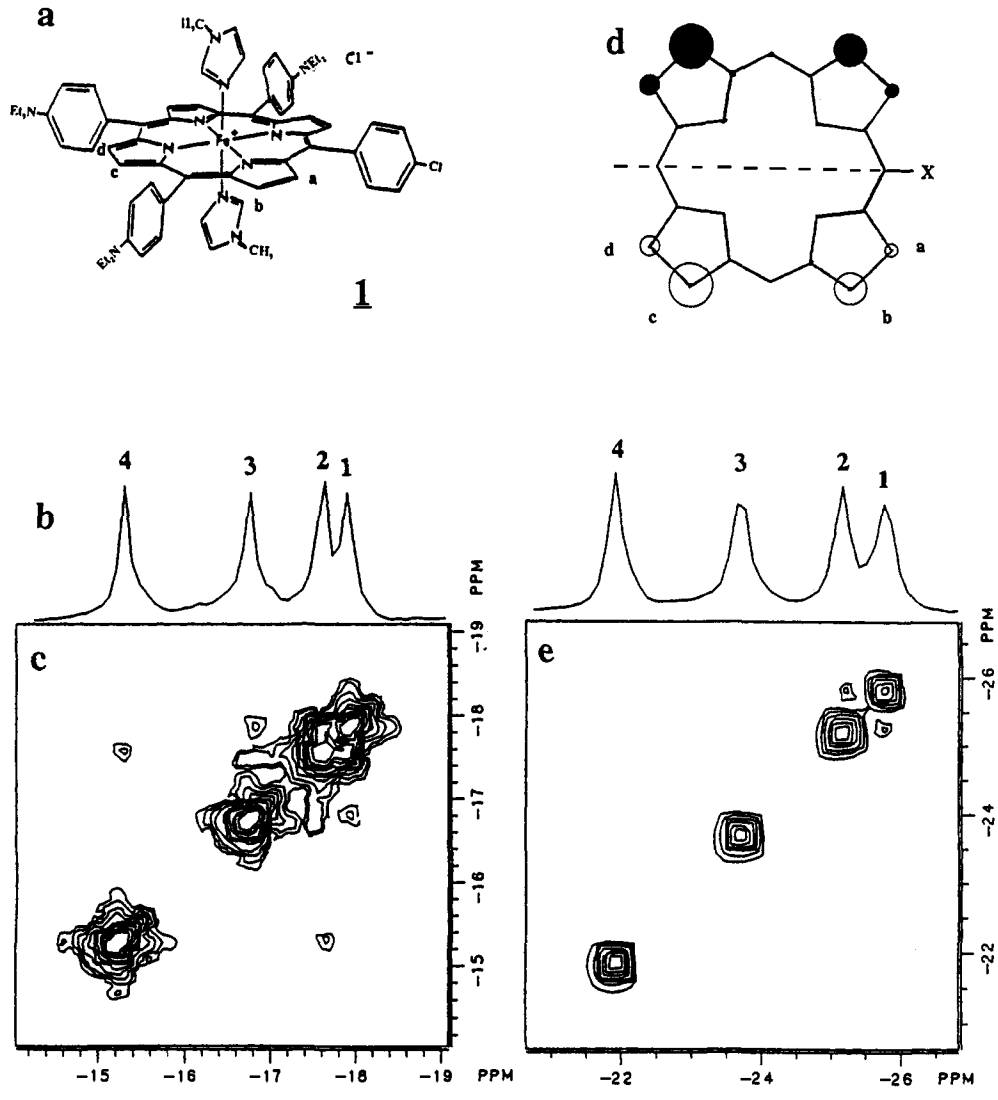

Figure 2. (a) Structure of $[(p\text{-Cl})(p\text{-NEt}_2)_3\text{TPPFe}(N\text{-MeIm})_2]\text{Cl}$ (**1**). (b) One-dimensional ^{1}H NMR spectrum of the pyrrole-H region of **1** at 21 °C. (c) COSY-45 spectrum of the pyrrole-H region of **1** at 21 °C. (d) Diagram of the β-pyrrole electron densities only in the higher-energy e(π) molecular orbital, which is preferred by **1** for unpaired electron spin delocalization (the sizes of circles represent the weighted averages of spin densities in the two similar-energy e(π) orbitals. (e) NOESY spectrum of the pyrrole-H region of **1**, recorded at −35 °C in CD_2Cl_2 with optimized mixing time of 6.2 ms.

As depicted in Figures 2b and 3b, the unique *p*-phenyl substituent creates four different electronic environments at the β-pyrrole carbon atoms which lead to four separate resonances for the eight protons attached to these positions, hereafter referred to as pyrrole protons and labeled H_a to H_d in Figures 2a and 3a. The four-peak pattern, which has been observed previously for other unsymmetrically substituted derivatives of $[\text{TPPFe}(N\text{-MeIm})_2]^+$,[26-28,30,31,33] clearly suggests that placing one unique substituent in the para position of one phenyl ring introduces a large perturbation of the unpaired electron spin density at the β-pyrrole positions. Such perturbation has previously been explained as arising from a redistribution of the π electron density and thus of unpaired electron spin density at the tetrapyrrole periphery.[17,27,28,56] The total spread of the four resonances due to the four types of protons, H_a–H_d, is 3.5–4.5 ppm, depending on temperature, and represents a sizable difference (roughly 30–40%) in the contact shifts of the protons that give rise to the most upfield and most downfield shifted pyrrole-H signals, *i.e.*, resonances labeled 1 and 4, respectively, in Figures 2b and 3b. In addition, the spacing of the resonances labeled 2 and 3 relative to 1 and 4 differs for the two complexes. We have suggested that the difference in spacing reflects the relative electron-withdrawing or -donating ability of the unique substituent,[28] and thus, as we will discuss below, the choice of the 3e(π) orbital preferred for unpaired electron spin delocalization.

Partial assignment of the four pyrrole proton resonances of **1** and **2** was achieved by a combination of ^{1}H COSY and NOESY investigations. The scalar couplings among the four protons labeled H_a,H_b and H_c,H_d for both **1** and **2** were deduced from the room temperature COSY maps depicted in Figures 2c and 3c. To determine which of the two modified e-symmetry molecular orbitals derived from those shown in Figure 1 is preferred for spin delocalization, through-space correlations between protons attached to carbon atoms that are not in the same pyrrole ring, observed in the NOESY spectra (Figures 2e and 3e), were analyzed. It should be noted that low-spin iron(III) tetraphenylporphyrinates have the shortest T_1 and T_2 values of any hemins of this spin state (~5–14 and 2–5 ms, respectively)

(56) La Mar, G. N.; Viscio, D. B.; Smith, K. M.; Caughey, W. S.; Smith, M. L. *J. Am. Chem. Soc.* **1978**, *100*, 8085.

(57) However, T_1 and T_2 values can be lengthened by 1–3 ms by removing (paramagnetic) dissolved dioxygen from the NMR samples, thereby increasing cross peak intensity and improving the quality of the 2-D maps to the level shown in Figures 2 and 3.

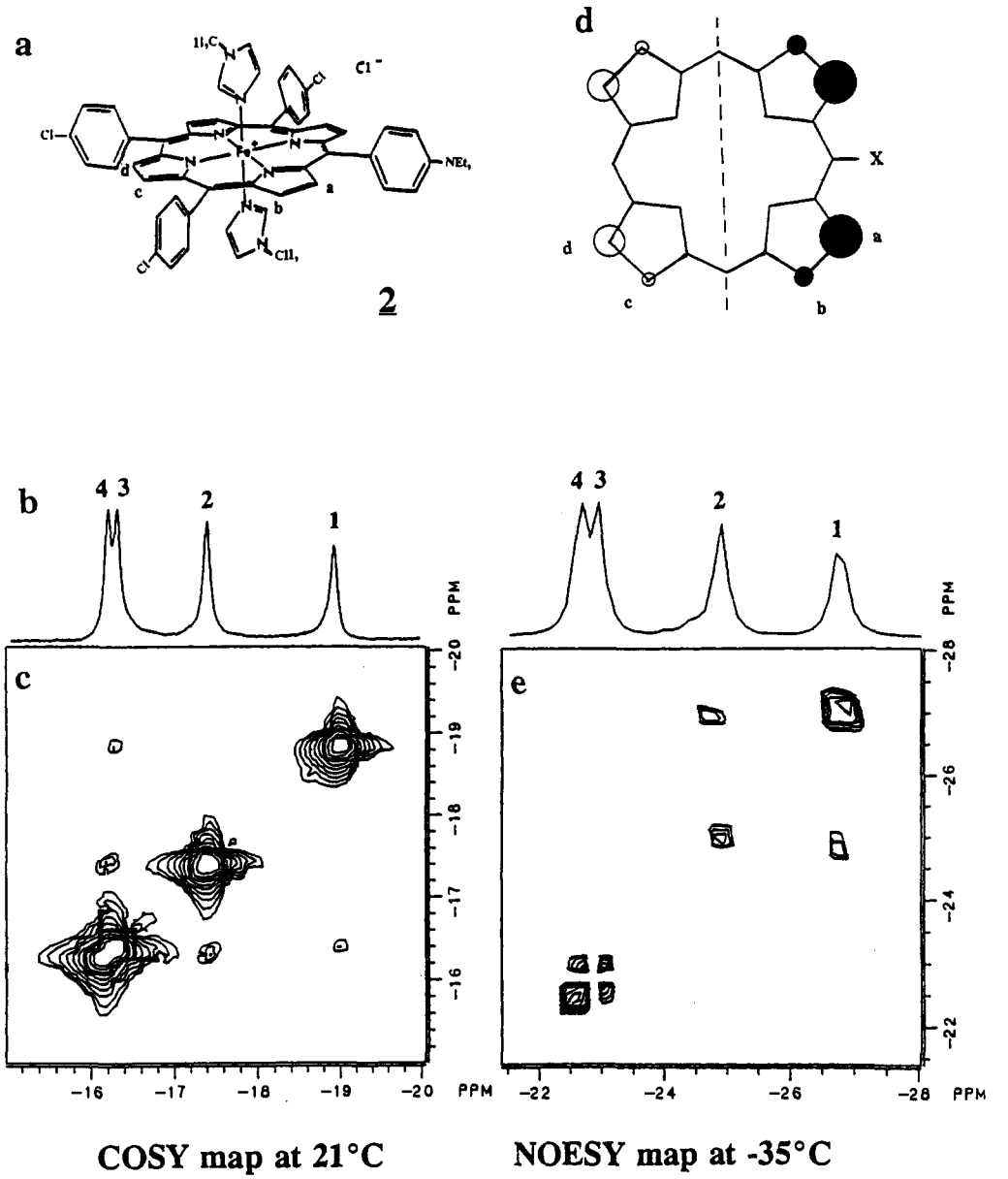

Figure 3. (a) Structure of $[(p\text{-}NEt_2)(p\text{-}Cl)_3TPPFe(N\text{-}MeIm)_2Cl$ (**2**). (b) One-dimensional ^1H NMR spectrum of the pyrrole-H region of **2** at 21 °C. (c) COSY-45 spectrum of the pyrrole-H region of **2** at 21 °C. (d) Diagram of the β-pyrrole electron densites only in the higher-energy e(π) molecular orbital, which is preferred by **2** for unpaired electron spin delocalization (the sizes of circles represent the weighted averages of spin densities in the two similar-energy e(π) orbitals. (e) NOESY spectrum of the pyrrole-H region of **2**, recorded at −35 °C in CD_2Cl_2 with optimized mixing time of 6.4 ms.

since the pyrrole protons are not "insulated" from the electron spin that is delocalized to the β-pyrrole carbons.[17] Hence, it is quite difficult to observe the COSY and NOESY cross peaks.[57] It is also worth mentioning that the NOESY data had to be acquired at −35 °C solely to suppress cross peaks due to chemical exchange, and not simply to increase the rotational correlation time τ_c. At room temperature, chemical exchange cross peaks between free and coordinated *N*-methylimidazole resonances are observed, and additional cross peaks are also observed among pyrrole protons that arise *via* the high-spin 5-coordinate intermediate in this chemical exchange process, as is discussed in greater detail elsewhere.[33] The additional cross peaks clearly diminish in intensity as the temperature is lowered, and they disappear at about −35 °C,[58] supporting the conclusion that a chemical exchange process is involved.

As is evident from Figure 2c, the COSY cross peaks between the pairs of resonances 1,3 and 2,4 indicate that resonances 1 and 3 are due to protons that are scalar coupled and are therefore in the same pyrrole ring, *i.e.*, either H_a and H_b or H_c and H_d, while resonances 2 and 4 are due to the protons in the other pyrrole ring. In the NOESY map of **1**, shown in Figure 2e, NOE cross peaks are observed only between resonances 1 and 2 at an optimized mixing time of 6 ms. Thus, the scalar coupled resonances due to H_a,H_b and H_c,H_d do not show NOESY cross peaks, as has also been found for other unsymmetrically substituted derivatives of $[TPPFe(N\text{-}MeIm)_2]^+$ investigated so far.[33] The absence of NOESY cross peaks from scalar coupled resonances suggests that the dominant cross-relaxation pathway in these paramagnetic complexes is due to mutual interaction of proton spins through bonds, where possible, rather than due to a through-

(58) Although NOESY cross peaks of these intermediate-sized molecules are expected to be stronger at lower temperatures due to increased molecular rotational correlation time, τ_c,[48] the quantity η/T, which is proportional to τ_c, changes by only about a factor of 2.5 for dichloromethane when the temperature is lowered from 21 °C to −35 °C, and hence the intensities of NOESY cross peaks were not detectably increased at −35 °C. (In fact, the intensities of the NOESY cross peaks diminished due to the shorter T_1 values at lower temperatures.) Although we could have chosen to use a solvent whose viscosity would have increased significantly at lower temperatures, the NOESY cross peak intensities of Figure 2e and 3e were sufficient for the purposes of this study. (The same may not be true for smaller model hemes, such as those based on the octaethylporphyrin ligand, or for many naturally occurring hemins.)

space dipolar pathway. This topic has been discussed at some length elsewhere.[33] However, more investigations of additional low-spin Fe(III) porphyrin complexes will be necessary in order to fully understand this phenomenon.

The strong cross peaks oberved in the NOESY map of **1** (Figure 2e) between resonances 1 and 2 can be explained by considering the nature of their chemical shifts. Resonances 1 and 2 have the most negative chemical shifts and thus have the largest isotropic and contact shifts of the four pyrrole protons.[15,17] The contact shift is the dominant contribution to the isotropic shift and is directly proportional to the unpaired electron spin density present in the p_π orbital of the carbon to which the proton is attached.[15,17] The relative spin densities ρ_C are related to the contact shifts of the protons of interest, δ_{con}:

$$A_H/h = (T\delta_{con})[3\gamma_H k/2\pi g\beta S(S+1)] = Q\rho_C/2S \quad (1)$$

where A_H is the Fermi contact coupling constant, γ_H is the magnetogyric ratio of the proton, g is the electronic g-factor, β is the Bohr magneton, S is the effective spin, $Q \approx -63$ MHz.[59] Hence, the proton that gives rise to resonance 1 in both Figures 2 and 3 has the largest contact shift and thus the carbon to which it is attached has the largest unpaired electron spin density. It can therefore be concluded that the NOESY spectrum (Figure 2e) identifies the protons attached to the carbons that have the largest unpaired electron spin density as being within 3–5 Å of each other.[48] This identifies resonances 1 and 2 as being due to H_c and H_b and defines the e-symmetry molecular orbital preferred for spin delocalization as that derived from the symmetrical e(π) orbital of Figure 1b, which has a node passing through the *meso* position carrying the unique substituent. It also suggests that for complex **1** the π unpaired electron spin density distribution in this orbital is modified as shown in Figure 2d.

This assignment is in excellent agreement with simple Hückel calculations, in which the energy of one *meso*-carbon p_π orbital is lowered with respect to the other three to simulate the inductive effect of an electron-withdrawing (electronegative) substituent. Similar empirical (but not arbitrary) adjustment of the energy of a carbon p_π orbital to simulate qualitatively the inductive effect of an electron-donating or -withdrawing substituent has been done as described by Streitwieser.[49] Even though very basic, these simple Hückel calculations predict that the electron density distribution in the highest-energy e-symmetry orbital (*i.e.*, the one that is half-filled) will be $\rho_{Cc} > \rho_{Cb} \gg \rho_{Cd} > \rho_{Ca}$, as shown in Figure 2d. This assignment is also consistent with the intuitive expectation that the most uniquely shifted resonance of both **1** and **2** is that due to the H_a type of pyrrole protons, *i.e.*, peak 4 for **1** and peak 1 for **2**.

Figure 3c shows the COSY spectrum of complex **2**. It can be seen that for this formula isomer, in which one phenyl ring bears an electron-donating para substituent relative to the other three, COSY cross peaks are again observed between the pairs of resonances 1,3 and 2,4, whereas the NOESY spectrum (Figure 3e) exhibits strong cross peaks between resonances 3 and 4 and weaker cross peaks between resonances 1 and 2. The strong cross peaks between resonances 3 and 4, which are due to the pyrrole protons with the smallest unpaired electron spin densities, identify the protons in near proximity to each other, *i.e.*, H_b and H_c, and thereby assign the π orbital preferred for unpaired electron spin delocalization as that derived from the one shown in Figure 1a. Simple Hückel MO calculations in which the energy of one *meso* carbon p_π orbital is raised with repect to the other three to simulate the inductive effect of an electron-donating (electropositive) substituent confirm that this orbital is preferred for unpaired electron spin delocalization and predict that the electron density distribution in the highest-energy e-symmetry orbital will be $\rho_{Ca} > \rho_{Cd} \gg \rho_{Cb} > \rho_{Cc}$, as shown in Figure 3e. The weaker cross peaks between resonances 1 and 2 observed in the NOESY spectrum of Figure 3e have also been obtained for other complexes that appear to use this π orbital[33] and suggest that when H_a and H_d are attached to carbon atoms having large spin density, cross peaks can be observed (probably by a mechanism different from that of a direct NOE), even though the distance is larger (~7 Å) than expected for proton–proton dipolar interactions.[48]

It should be noted that the present COSY and NOESY investigations do not yet provide an *absolute* assignment of H_a–H_d, since we cannot *positively* assign which of the two resonances 3 and 4 of **1** or 1 and 2 of **2** is due to H_a and which to H_d. This is because, to date, we have not been able to detect cross peaks between the ortho H of the phenyl rings (including the unique phenyl ring) and any of the pyrrole proton resonances (data not shown). We believe that the very large difference in T_1 of the pyrrole-H and phenyl-H (~12 as compared to ~200 ms, respectively), as well as the partial rotational motion of the phenyl rings, has probably inhibited the detection of such cross peaks. However, it seems logical to assign the most uniquely shifted resonance (peak 4 for **1** and peak 1 for **2**) to H_a. This is equivalent to saying that the most isotropically shifted resonance (peak 1) is due to H_c for **1** and H_a for **2**, because once one pyrrole-H resonance is assigned unambiguously, the cross peaks observed in the COSY and NOESY spectra of Figures 2 and 3 provide unambiguous assignment of the remaining resonances. And although simple Hückel calculations suggest that for **1**, resonance 1 should be due to H_c, the 2-D NMR cross peak patterns of Figure 2c,e are consistent not only with this assignment but also with resonance 1 being due to H_b. Although this ambiguity does not affect the conclusion that it is the orbital of Figure 1b that is preferred for spin delocalization, it does change the precise details of the modification of that orbital by the inductive effect of the unique *p*-Cl-phenyl substituent. The synthesis of additional low-spin Fe(III) porphyrinates, in which an ortho CH_2 substituent is present on one phenyl ring, may allow us to connect the phenyl and pyrrole spin systems by NOESY techniques.[60]

The major accomplishment of this work is that the cross peak patterns observed in the 2-D maps of Figures 2 and 3 allow us to determine unambiguously which π molecular orbital is preferred for spin delocalization for complexes **1** and **2**, and again it should be stressed that even simple Hückel calculations support the assignments. When a relatively electron-withdrawing substituent is present on one of the phenyl rings, as in **1**, the π orbital preferred for spin delocalization is the one with small electron density at the β-pyrrole carbons closest to and most distant from the unique substituent (Figure 1b). In contrast, when a relatively electron-donating substituent is present, as in **2**, the preferred π molecular orbital has large electron density at the closest and most distant β-pyrrole carbons (Figure 1a). Although this might seem counterintuitive at first glance, it should be noted again that in these bis(*N*-methylimidazole) complexes, low-spin Fe(III) has the electron configuration $(d_{xy})^2(d_{xz},d_{yz})^3$.[15,17] Thus, for **1**, the interaction of the e(π) and d_π orbitals of Figure 1a,b produces two low-energy e-symmetry MOs that are mainly porphyrin π in character and are filled and two high-energy (valence) orbitals that are mainly metal in character and contain three electrons. Of these valence molecular orbitals, the modified e-symmetry molecular orbital derived from that shown in Figure 1a, which has *large* electron density at C_a, is shifted to lower energy by the electron-withdrawing substituent and is thus filled. On the other hand, the e-symmetry molecular orbital derived from that shown in Figure 1b, which has *small* electron density at C_a, is not shifted in energy by the electron-withdrawing substituent, so it is relatively higher in energy than the orbital of Figure 1a and is thus half-filled. This leads to the observed pattern of pyrrole-H resonance shifts, $|\delta_{Ha}| \sim |\delta_{Hd}| \ll |\delta_{Hb}| \sim |\delta_{Hc}|$. In contrast, for complex **2**, the relative energies of the two modified e-symmetry valence molecular orbitals are reversed (again, the valence orbital derived from that of Figure 1b is not shifted in energy, but the one derived

(59) McConnell, H. M. *J. Chem. Phys.* **1956**, *24*, 764.

(60) Tarr, D. A.; Simonis, U.; Walker, F. A., work in progress.

from that shown in Figure 1a is shifted to higher energy), and thus the half-filled π molecular orbital is that derived from the one shown in Figure 1a, leading to the observed order of pyrrole-H shifts, $|\delta_{Ha}| \sim |\delta_{Hd}| \gg |\delta_{Hb}| \sim |\delta_{Hc}|$. The important point here is that the *reversal in energy* of the two e-symmetry valence molecular orbitals derived from those shown in Figure 1 when one electron-donating group on one meso position is replaced by an electron-withdrawing group, or vice versa, determines the observed pattern of large and small isotropic shifts of the protons $H_a - H_d$.

Since the actual difference in energy of the two e-symmetry molecular orbitals of **1** and **2** is likely only of the order of several tens of cm^{-1}, it is expected that at the temperatures of the NMR investigations, both orbitals are fractionally utilized for spin delocalization, but to differing extents as the temperature is varied. This is clearly seen by comparing the chemical shifts of the pyrrole protons of **1** and **2** at +21 °C and −35 °C in Figures 2b,e and 3b,e, respectively, and the relative sizes of the circles of Figures 2d and 3d are presented with this fractional utilization in mind. In the future, more sophisticated molecular orbital calculations may allow not only quantitation of the electron density distribution in the two e(π) valence molecular orbitals but also an estimation of the likely energy difference between them. Such calculations are currently in progress in our laboratories.

In conclusion, the cross peak patterns observed in the COSY and NOESY maps presented in Figures 2 and 3, in combination with the modeling of the unpaired electron spin density distributions for these para-substituted derivatives of [TPPFe(*N*-MeIm)$_2$]$^+$, can be unambiguously correlated to the relative electronic effects of the two types of substituents present, thereby allowing the electron-donating/withdrawing effects of other substituents, including ortho substituents,[30,33] for which no Hammett σ constants are available, to be assigned in the future. Hence, two-dimensional ^{1}H NMR investigations, in combination with the calculated electron density distribution pattern in the modified e(π) valence molecular orbitals, may yield information concerning the electron-donating or -withdrawing characteristics of *o*-phenyl substituents. Such information is not only important for understanding the effects of substituents on the molecular orbitals of the porphyrin ring but is also very important for understanding the electronic effects of *o*-phenyl substituents in general and the roles they may play in the reactivity of models of the cytochromes P450.[61-64]

In addition to the information provided concerning the effect of phenyl substituents on the modification of the electron density distribution in the e-symmetry π orbitals of the model hemes discussed herein and others to which they are structurally related, the present studies may provide a useful way for explaining the distribution of unpaired electron spin densities in other synthetic and naturally occurring hemes in which the porphyrin ring has been modified by chemical reactions that cause substitution of an electronegative or electropositive atom or group on the heme ring. Examples of such systems include the products of the natural breakdown of heme by the enzyme heme oxygenase,[51] in which the heme is attacked at one of the *meso*-carbons by dioxygen to produce oxophlorins,[65,66] verdohemins,[66b] the iron complexes of biliverdin,[66c] and/or monoazahemins.[66d] Each of these macrocyclic complexes of iron(III) shows distinctive NMR spectra indicative of anisotropic unpaired electron spin delocalization within the π system of the macrocycle that could be mapped by COSY and NOESY techniques and molecular orbital calculations. Likewise, model hemes in which either a *meso*-carbon or a β-pyrrole carbon have undergone either nucleophilic attack on the Fe(III) porphyrin cation radical[67] or electrophilic attack on the Fe(II) anion radical[68] by some heteroatom or group (NO_2,[67] PPh_3,[67] Br[68]) also show anisotropic unpaired electron spin delocalization[67] that could be mapped and quantified by use of the types of two-dimensional NMR experiments described herein in combination with molecular orbital calculations. The approach described in this paper, with a more sophisticated level of calculations, may lead to a more complete understanding of the effect of the heteroatom on the distribution of electron density and hence spin density in the π system of the modified macrocycle.

In addition to information obtainable for simple hemes, our strategy of combining 2-D NMR spectroscopy and molecular orbital modeling has been essential for proposing a model for the mechanism of action of the enzyme heme oxygenase.[51] When its natural substrate, hemin, is bound to the enzyme as the low-spin monocyano complex, the heme substituent protons have recently been reported to show large anisotropic π unpaired electron spin delocalization analogous to the patterns observed for **1** and **2**, presumably due to the close proximity of reactive protein side chains poised to attack the heme.[52] By consideration of our approach of raising or lowering the energy of the α-*meso*-carbon p_π orbital to simulate the inductive effect of this reactive side chain, it has been possible to model the electronic effect of this as yet unidentified reactive protein side chain on the observed isotropic shifts of the heme substituents. On the basis of this approach, it has been postulated that the reactive group must be electrophilic rather than nucleophilic.[52]

Acknowledgment. The financial support of National Institutes of Health Grant DK 31038 is gratefully acknowledged. The Department of Chemistry and Biochemistry at San Francisco State University also acknowledges grants from the National Institutes of Health (RR 02684) and the National Science Foundation (DMB-8516065) for purchase of the NMR spectrometers. The authors also wish to acknowledge stimulating conversations with Professor G. N. La Mar concerning the NMR spectra of the heme oxygenase enzyme prior to submission of this manuscript for publication and to thank him for providing a copy of the submitted manuscript.

Supplementary Material Available: Table SI, calculated simple Hückel MO coefficients for **1** and **2**; Table SII, semiquantitative comparison of contact shifts and Hückel MO coefficients (3 pages). This material is contained in many libraries on microfiche, immediately follows this article in the microfilm version of the journal, and can be ordered from the ACS; see any current masthead page for ordering information.

(61) Ortiz de Montellano, P. R., Ed. *Cytochrome P-450, Structure, Mechanism and Biochemistry*; Plenum: New York, 1986.
(62) Ortiz de Montellano, P. R. *Acc. Chem. Res.* **1987**, *20*, 289.
(63) Gunter, M. J.; Turner, P. *Coord. Chem. Rev.* **1991**, *108*, 115.
(64) Mansuy, D.; Battioni, P. In *Bioinorganic Catalysis*; Reedijk, J., Ed.; Marcel Dekker: New York, 1993; p 395.
(65) (a) Gold, A.; Ivey, W.; Toney, G. E.; Sangaiah, R. *Inorg. Chem.* **1984**, *23*, 2932. (b) Masuoka, N.; Itano, H. A. *Biochemistry* **1987**, *26*, 3672.
(66) (a) Balch, A. L.; Latos-Grazynski, L.; Noll, B. C.; Olmstead, M. M.; Zovinka, E. P. *Inorg. Chem.* **1992**, *31*, 2248. (b) Balch, A. L.; Latos-Grazynski, L.; Noll, B. C.; Olmstead, M. M.; Szterenberg, L.; Safari, N. *J. Am. Chem. Soc.* **1993**, *115*, 1422. (c) Balch, A. L.; Olmstead, M. M.; Safari, N. *Inorg. Chem.* **1993**, *32*, 291. (d) Balch, A. L.; Latos-Grazynski, L.; Noll, B. C.; Olmstead, M. M.; Safari, N. *J. Am. Chem. Soc.* **1993**, *115*, 9056.
(67) Malek, A.; Latos-Grazynski, L.; Bartczak, T. J.; Dadlo, A. *Inorg. Chem.* **1991**, *30*, 3222.
(68) Callot, H. J. *Bull. Soc. Chim. Fr.* **1974**, 1492.